Optical Materials EXPRESS

is how nonlocality affects absorption in the quantum regime, specifically whether the presence of a single photon at a point $\boldsymbol{r}_1$ can influence the absorption of a second photon at another point $\boldsymbol{r}_2$. Additionally, the "reverse LD", or luminescence of metallic structures, warrants further investigation, particularly regarding the spatial and angular distribution of emitted photons and polaritons. It is hoped that future research will uncover more phenomena with potential practical applications.

5. Landau damping of surface plasmons in metal nanoparticles: the RPA approach

TIGRAN V. SHAHBAZYAN

Overview

There has been a renewed interest in the role of nonlocal phenomena in optical response of metal-dielectric structures [14,64,108]. *Landau damping* (LD) of localized surface plasmons (LSP) is one of the earliest manifestations of nonlocal effects observed as broadening of the LSP resonance in optical spectra of small metal nanoparticles (NP) [103]. The optically excited LSP decays into single-particle excitations while momentum matching is provided by the electron scattering off the confining potential. For small NPs, this momentum relaxation mechanism can be incorporated, along with the bulk phonon and impurity scattering, into Drude's dielectric function of the metal $\varepsilon(\omega) = \varepsilon_\infty - \omega_p^2/\omega(\omega + i\gamma)$, where ω_p is the plasma frequency, and γ is the scattering rate. The latter is presented as the sum $\gamma = \gamma_0 + \gamma_s$ of bulk scattering rate γ_0 and of surface-induced rate

$$\gamma_s = A\frac{v_F}{L}, \tag{18}$$

where v_F is the electron Fermi velocity, L is NP's characteristic size, and A is a phenomenological constant in the range 0.3–1.5 accounting for surface-related effects [103].

Current status

The scattering rate γ_s was initially associated with electron's classical scattering (CS) time $\tau_{cs} = L/v_F$ across the NP [109,110], but later it was recognized as intrinsically nonlocal effect. An alternating electric field excites an electron-hole (e-h) pair with energy $\hbar\omega$ across the Fermi level E_F. For typical LSP energies $\hbar\omega \ll E_F$, such a process requires momentum transfer $q = \hbar\omega/v_F$, facilitated by surface scattering, which defines nonlocal length scale $\xi = \hbar/q = v_F/\omega$ [64]. For common plasmonic metals such as gold (Au) and silver (Ag), this scale is below 1 nm (e.g., for Au, $\xi \approx 0.5$ nm at wavelength $\lambda = 700$ nm), implying that e-h pair excitation takes place in the close proximity ξ to the metal surface (see Fig. 7). For a NP with characteristic size L, the probability of such process occurring during the optical cycle is $\sim \omega\xi/L$, leading to Eq. (18). Despite subnanometer scale of ξ, the broadening of optical spectra associated with γ_s has been observed for NPs of various shapes with sizes up to $\sim$ 10 nm. In the presence of surface scattering, the LSP resonance quality factor is $Q = \omega/\gamma \approx Q_0/[1 + (\xi/L)Q_0]$, where $Q_0 = \omega/\gamma_0$, implying that nonlocal effects in plasmonics persist at much larger scale $L \sim \xi Q_0 \gg \xi$.

For spherical NPs in the size range transitioning from metal clusters to several nm, calculations within jellium model using time-dependent local-density approximation (TDLDA) highlighted the important role of electron confining potential and electron density spillover beyond the NP classical boundary [111,112]. At the same time, for larger NPs in the size range above several nanometers, TDLDA calculations revealed that the precise shape of confining potential is largely unimportant and the overall magnitude of γ_s, defined by the coefficient A, is determined by the electron spillover and dielectric environment effects [113,114]. The reasonable accuracy of Eq. (18) even for relatively large NPs indicates that, for $L \gg \xi$, the LD rate γ_s can be obtained as

Optical Materials EXPRESS

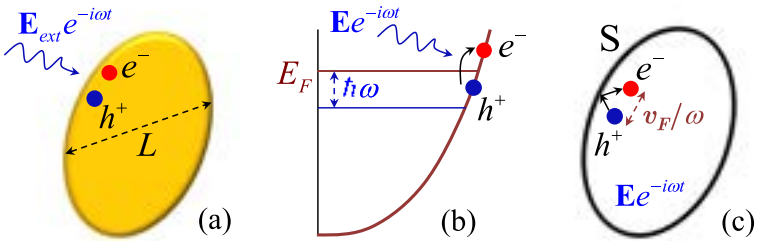

Fig. 7. Schematics for surface-assisted excitation of an *e-h* pair with energy $\hbar\omega$. (a) An external optical field incident on a metal nanostructure of characteristic size L, (b) excites LSP that decays into an *e-h* pair, (c) with momentum matching provided by carrier surface scattering in a region of size v_F/ω.

a correction to the Drude dielectric function within a standard analytical approach such as the random-phase approximation (RPA) and the Lindhard dielectric function [9].

RPA calculations of γ_s have been carried out in the course of several decades [100–102, 115–119]. While in earlier studies, the scattering rate for *spherical* NPs with radius a was derived as $\gamma_{sp} = 3v_F/4a$, the subsequent works focused on obtaining γ_s for NPs of more complex shapes. The major challenge was to obtain the LD rate for NPs of *arbitrary* shape, even irregular one, for which no numerical calculations are feasible. The condition $L \gg \xi$ implies that the length scales for electronic and LSP excitations are well separated. For hard-wall confining potential, the electronic contribution to γ_s can be effectively "integrated out" and the LD rate is obtained as a *nonlocal* correction to the Drude decay rate as $\gamma = \gamma_0 + \gamma_s$, where γ_s has the form 18 with the characteristic size L depending on the field distribution in the metal [100–102]:

$$L = \frac{\int dV\, |\boldsymbol{E}|^2}{\int dS\, |E_n|^2}. \tag{19}$$

Here, $\boldsymbol{E}$ is the electric field inside a NP of volume V, E_n is the field component *normal* to the NP surface S, and $A = 3/4$. Importantly, γ_s is sensitive to *polarization* of the LSP field that drives the electrons towards the interface. Such form of L (and γ_s) is valid for NPs in the size range $\xi \ll L \ll \lambda$, where λ is the optical wavelength, which includes most plasmonic systems used in the applications.

RPA approach to Landau damping in small metal nanoparticles. Here we briefly outline the RPA approach to LD of LSP in metal NPs following Refs. [101,102]. An external field excites an LSP in a NP which subsequently decays into an *e-h* pair by promoting, with its alternating field $\boldsymbol{E}e^{-i\omega t}$, a conduction band electron across the Fermi level, while the momentum matching is provided by carriers' surface scattering (see Fig. 7). The full dissipated power Q in a metal NP is given by

$$Q = \frac{\omega}{2}\,\mathrm{Im}\int dV\, \boldsymbol{E}^* \cdot \boldsymbol{P}, \tag{20}$$

where $\boldsymbol{P}(\boldsymbol{r})$ is the electric polarization vector (the star stands for complex conjugation). The bulk contribution to Q is obtained by relating, in the *local* limit, the polarization vector to the electric field as $\boldsymbol{P}(\boldsymbol{r}) = \boldsymbol{E}(\boldsymbol{r})[\varepsilon(\omega) - 1]/4\pi$, yielding the standard expression

$$Q = \frac{\omega\varepsilon''(\omega)}{8\pi}\int dV\, |\boldsymbol{E}|^2, \tag{21}$$

where $\varepsilon''(\omega)$ is the imaginary part of metal dielectric function due to bulk relaxation processes. For small NPs, there is also a surface contribution Q_s to the dissipated power arising from momentum relaxation due to surface scattering. The general expression for Q_s is obtained by

Optical Materials EXPRESS

relating $\boldsymbol{P}(\boldsymbol{r})$ to *nonlocal* electron polarization operator $\Pi(\omega;\boldsymbol{r},\boldsymbol{r}')$ via the induced charge density $\rho(\boldsymbol{r})$ as

$$\boldsymbol{\nabla}\cdot\boldsymbol{P}(\boldsymbol{r}) = -\rho(\boldsymbol{r}) = -e\int dV'\,\Pi(\omega;\boldsymbol{r},\boldsymbol{r}')\Phi(\boldsymbol{r}'). \tag{22}$$

Here, the potential $\Phi(\boldsymbol{r})$ is defined as $e\boldsymbol{E}(\boldsymbol{r}) = -\boldsymbol{\nabla}\Phi(\boldsymbol{r})$, where e is the electron charge. Using Eq. (22), after integrating Eq. (20) by parts, the dissipated power takes the form

$$Q_s = \frac{\omega}{2}\mathrm{Im}\int dV dV'\,\Phi^*(\boldsymbol{r})\Pi(\omega;\boldsymbol{r},\boldsymbol{r}')\Phi(\boldsymbol{r}'), \tag{23}$$

where $\Pi(\omega;\boldsymbol{r},\boldsymbol{r}')$ includes only the electronic contribution. Within RPA, $\Pi(\omega;\boldsymbol{r},\boldsymbol{r}')$ is replaced by the polarization operator for noninteracting electrons, yielding

$$Q_s = \pi\omega\sum_{\alpha\beta}|M_{\alpha\beta}|^2\left[f(\epsilon_\alpha) - f(\epsilon_\beta)\right]\delta(\epsilon_\alpha - \epsilon_\beta + \hbar\omega), \tag{24}$$

where $M_{\alpha\beta} = \int dV\psi_\alpha^*\Phi\psi_\beta$ is the transition matrix element of potential $\Phi(\boldsymbol{r})$ calculated from the wave functions $\psi_\alpha(\boldsymbol{r})$ and $\psi_\beta(\boldsymbol{r})$ of electron states with energies ϵ_α and ϵ_β separated by $\hbar\omega$, $f(\epsilon)$ is the Fermi distribution function, and spin degeneracy is included. For NPs of arbitrary shape, a direct numerical evaluation of $M_{\alpha\beta}$ is not possible due to complexity of the electron wave functions. However, for NPs with characteristic size $L \gg \xi$, this issue can be bypassed by extracting the *surface* contribution to the matrix element as [101]

$$M^s_{\alpha\beta} = \frac{-e\hbar^4}{2m^2\epsilon^2_{\alpha\beta}}\int dS\,[\nabla_n\psi_\alpha(\boldsymbol{s})]^* E_n(\boldsymbol{s})\nabla_n\psi_\beta(\boldsymbol{s}), \tag{25}$$

where $\nabla_n\psi_\alpha(\boldsymbol{s})$ is wave function's derivative normal to the surface, $E_n(\boldsymbol{s})$ is the corresponding normal field component, $\epsilon_{\alpha\beta} = \epsilon_\alpha - \epsilon_\beta$ is the *e-h* pair excitation energy, and m is the electron mass. The integration in Eq. (25) takes place over the NP surface S, while the volume contribution to the matrix element is negligibly small due to near-vanishing overlap of the electron wave-functions in the presence of slowly varying potential Φ. Using this expression for the matrix element, the surface contribution to the dissipated power (24) can be recast as

$$Q_s = \int\int dS dS'\,E_n(\boldsymbol{s})E^*_{n'}(\boldsymbol{s}')F(\boldsymbol{s},\boldsymbol{s}'), \tag{26}$$

where $F(\boldsymbol{s},\boldsymbol{s}')$ is the *e-h* correlation function, which is expressed via normal derivatives of the electron and hole Green functions in a hard-wall cavity (see Ref. [101]).

Evaluation of Q_s hinges on the observation that excitation of an *e-h* pair with energy $\hbar\omega$ takes place in a region of size $\sim\xi \ll L$. Then it can be shown that $F(\boldsymbol{s},\boldsymbol{s}')$ peaks in the region $|\boldsymbol{s}-\boldsymbol{s}'| \sim \xi$ and rapidly oscillates outside of it. Since the electric field is relatively smooth on the scale L, the *e-h* correlation function can be approximated by $F(\boldsymbol{s},\boldsymbol{s}') = F_0\,\delta(\boldsymbol{s}-\boldsymbol{s}')$, where the coefficient F_0 is evaluated using single-scattering approximation for the electron Green function as $F_0 = (3v_F\omega_p^2/32\pi\omega^2)$ [101]. The final expression for the surface-induced dissipated power has the form

$$Q_s = \frac{3v_F}{32\pi}\frac{\omega_p^2}{\omega^2}\int dS\,|E_n|^2. \tag{27}$$

Comparing Q_s with the bulk expression (21), one observes that both contributions can be combined together by adding an imaginary nonlocal correction $\delta\varepsilon_s$, where

$$\delta\varepsilon_s = i\frac{\omega_p^2\gamma_s}{\omega^3}, \quad \gamma_s = \frac{3v_F}{4}\frac{\int dS\,|E_n|^2}{\int dV\,|\boldsymbol{E}|^2}, \tag{28}$$

to the Drude bulk dielectric function. The above form for $\delta\varepsilon_s$ implies that the scattering rate in the Drude dielectric function $\varepsilon(\omega)$ should be modified as $\gamma = \gamma_0 + \gamma_s$. A similar expression for γ_s was obtained in Ref. [100] using a different approach.

Optical Materials EXPRESS

Although γ_s is independent of the electric field's overall amplitude, it is highly sensitive to field's polarization that defines the electrons motion relative to the metal–dielectric interface. In the case of asymmetric NPs, such polarization dependence implies that the LD rate can vary significantly for *different* LSP modes excited in the *same* system. This point is illustrated in Fig. 8 for longitudinal (L) and transverse (T) modes in nanorods and nanodisks, modeled by the prolate (P) and oblate (O) spheroids, respectively. For such systems, explicit analytic expressions for the LD rate has been obtained in the form [101] $\gamma_s = \gamma_{\rm sp} f_{L,T}$, where

$$f_L = \frac{3}{2\tan^2(\alpha)}\left[\frac{2\alpha}{\sin(2\alpha)} - 1\right], \quad f_T = \frac{3}{4\sin^2(\alpha)}\left[1 - \frac{2\alpha}{\tan(2\alpha)}\right]. \tag{29}$$

Here, for a prolate spheroid (nanorod), $\alpha = \arccos(b/a)$, where a and b are semi-major and semi-minor axis respectively, while for an oblate spheroid (nanodisk), the LD rates have the same form 29 but with $\alpha = i\,\mathrm{arccosh}(b/a)$. For comparison, the CS model rate $\gamma_{\rm cs} = v_F S/4V$, which is independent of mode polarization, is also plotted in Fig. 8. For visual convenience, all rates are normalized by the LD rate $\gamma_{\rm sp} = 3v_F/4a$ for a spherical NP of radius a. At the sphere point $a = b$, the normalized rates continuously transition into each other (e.g., PL to OL and PT to OT), but away from it, the rates for different modes exhibit dramatic difference in magnitude depending on the mode polarization.

Discussion and further developments

The surface scattering rate Eq. (28) quantifies LD in "simple" NPs characterized by a single metal surface. Further developments involved more complex plasmonic systems such as thin films [120], core-shell hybrid structures [121–123] and NP dimers [106,124]. In thin films or metal nanoshells with dielectric core, the surface scattering that accompanies *e-h* pair excitation can take place from *both* the inner and outer metal boundaries. The interference between these processes can lead to *coherent* oscillations (quantum beats) of γ_s with changing metal thickness d. Such oscillations were reported in TDLDA studies of thin Ag films [120] and later in RPA calculations of γ_s for spherical metal nanoshells [121,122]. Specifically, for metal nanoshells with thickness d, the LD rate acquires an interference-induced contribution $\gamma_s^{\rm int} \approx B\sin(d/\xi)$ where the coefficient B depends on the nanoshell's thickness and overall size [122].

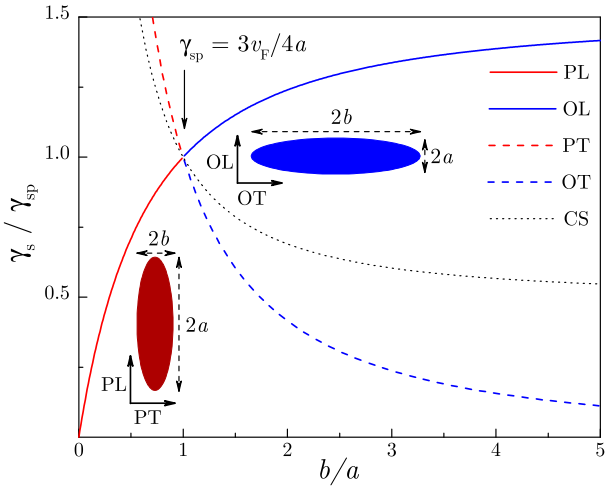

Fig. 8. Normalized surface scattering rates for prolate and oblate spheroids along with the CS rate are plotted against aspect ratio b/a. Insets: Schematics of LSP modes.

Optical Materials EXPRESS

In plasmonic dimers, LD has been shown to play a critical role in limiting the field enhancement in the gap between closely spaced NPs [106,124]. Numerical calculations of the field intensity performed within RPA using the Lindhard dielectric function [106] and within the generalized nonlocal optical response (GNOR) model [124] revealed a significant increase in the LD rate that reduced the field enhancement factor in the gap by nearly two orders of magnitude. Qualitatively, the LD rate increase for narrow gaps can be inferred from the characteristic size L, given by Eq. (19), which depends on the field distribution inside the metal. Note that, in the absence of electron wave-function overlap between two NPs, excitation of an *e-h* pair can take place in either NP, so that the LD rate for a dimer is the sum of individual NP LD rates. In dimers, the field intensity is highest in the gap between the NPs and is much weaker in the metal, where it is concentrated in a relatively small volume around the gap. More precisely, the integrated LSP density of states (DOS) $\rho(\omega)$ can be split into contributions from the regions *inside* the metal and *outside* of it as $\rho(\omega) = \rho_{\rm in}(\omega) + \rho_{\rm out}(\omega)$, with their relative magnitude $\rho_{\rm out}(\omega)/\rho_{\rm in}(\omega) = |\varepsilon'(\omega)| \gg 1$, where $\varepsilon'(\omega)$ is the real part of metal dielectric function [125]. With decreasing NP separation, as the LSP resonance redshifts [106,124], this ratio increases with $|\varepsilon'(\omega)|$ implying that the electric field is further pushed out from the metal into the gap. As a result, the volume-integrated field intensity in the numerator of Eq. (19) decreases relative to the surface-integrated intensity in the denominator, leading to a reduced L and, hence, enhanced LD rate for narrow gaps.

The overall magnitude of the LD rate 18 is defined by the coefficient A that depends on the electron confining potential and charge density profile, which, in turn, determine the electric fields near the interface. Recent TDLDA calculations for relatively large (up to 10 nm) NPs [113,114] indicate that the main impact on the LSP resonance width comes from the electron density spillover and dielectric environment, rather than the electronic states in the cavity. Since the electron spillover is not sensitive to the overall NP shape, the TDLDA value $A \approx 0.32$ for a nanosphere [113,114] is likely shape independent. Note, however, that substantially larger values in the range 0.3–1.5 were reported in the experiment depending on the surrounding dielectric medium [103]. On the other hand, the presence of d-band electrons with a nearly step-like density profile in noble-metals gives rise to a thin surface layer, in which the conduction electrons with extended density tail are no longer screened by the d-band electrons, which leads to the field enhancement near the interface [126]. In Ag NPs, this effect has been shown to cause a blueshift of the LSP resonance which, in fact, overcompensates the resonance redshift due to the electron density spillover [127]. One can expect that a similar competition between these two nonlocal mechanisms will take place for the LD rate as well and bring the coefficient A closer to the experiment. A related effect has been recently studied for Ag NPs coated with a thin dielectric shell [123]. In this case, the electron spillover into a medium with a much weaker field screening results in a noticeable LD rate enhancement.

Concluding remarks

In this contribution, we tried to present a brief outlook on the Landau damping (LD) of surface plasmons in metal nanoparticles (NPs). This phenomenon has attracted a constant interest for over 50 years due to its prominent role in the optical spectra of small NPs. There is a very extensive literature on LD in NPs, and several theoretical and numerical approaches have been developed during this time span. We have focused on recent advances within the RPA approach which resolved a long-standing problem of describing, by means of a relatively simple analytical model, the LD of surface plasmons in metal NPs of arbitrary shape. On the applications side, LD is an efficient source of hot electrons widely used in photochemistry and light harvesting; there are excellent reviews on this topic the readers are referred to.

Funding. National Science Foundation (DMR-2000170, DMR-2301350, NSFPREM-2423854).